JOURNAL OF Materials CHEMISTRY

The surface characterisation of coated titanium dioxide by FTIR spectroscopy of adsorbed nitrogen

Terry A. Egerton* and Ian R. Tooley

Physical Chemistry Department, Bedson Building, Newcastle University, Newcastle Upon Tyne, UK NE1 7RU. E-mail: T.A.Egerton@ncl.ac.uk

Received 4th July 2001, Accepted 17th January 2002
First published as an Advance Article on the web 19th February 2002

Infrared (IR) absorption, at 2335 cm^{-1}, of nitrogen adsorbed on high area titanium dioxide samples has been measured for both untreated TiO_2 and for two series of samples prepared by precipitating an inorganic coating on the same parent rutile. The intensity of the absorption, at 2335 cm^{-1} progressively decreases as the amount of inorganic coating increases, *i.e.* as the probability of 'bare', uncoated, titanium dioxide surface decreases. For both oxides the nitrogen band is eliminated, *i.e.* the rutile surface is completely covered, by $\sim$30% w/w oxide coating. This corresponds to $\sim$0.2% of oxide per square metre of rutile. However, at lower coating levels, silica coating reduces adsorption of IR-active nitrogen more effectively than the same weight of alumina. Rates of propan-2-ol photo-oxidation to acetone have also been measured on the uncoated and coated rutiles used for the nitrogen studies. The pattern of decreased activity as a function of the amount of coating broadly follows the decrease in the nitrogen band intensity. Therefore, we conclude that the surface sites associated with the adsorption of IR-active nitrogen are closely associated with the sites responsible for photo-oxidation.

Introduction

This paper describes the use of infrared (IR) spectroscopy of adsorbed nitrogen to characterise inorganic coatings on TiO_2. Titanium dioxide, in the form of $\sim$200 nm microcrystals, is the dominant white pigment, with world sales of 4 Mt $annum^{-1}$.[1] More recently, 'ultrafine' titanium dioxide with mean particle size below 100 nm has found increasing application as an inorganic sun block in high efficacy sun creams.[2] In both applications the surface properties of the titanium dioxide are usually modified by application of an inorganic coating, typically based on hydrous oxides, or phosphates, of silicon or aluminium.[3–7] Recently, inorganic coatings have been exploited more widely, both technologically, *e.g.* in ceramics,[7] and in fundamental studies, *e.g.* for silica encapsulation of quantum dots and metal clusters.[8]

In the specific context of titanium dioxide, coatings based on alumina[4,6] are usually used to control the dispersion properties[4,5] of the TiO_2 in the medium of use.[5] (For the sake of simplicity, coatings based on, *e.g.*, hydrous oxides of aluminium or silicon will be referred to as alumina or silica for the rest of this paper. This is simply a convenient short-hand—it does not imply a specific stoichiometry or crystalline structure.) A second coating type, based on a dense silica layer,[3] is particularly important in reducing the TiO_2 photoactivity. Photoactivity results from photogeneration of highly reactive hydroxyl radicals at the crystal surface,[9,10] and is undesirable in pigments because it leads to photocatalytic destruction of surrounding organics, *e.g.* paint films, leading ultimately to complete oxidation to carbon dioxide.[11] Similarly, even though the cells in the layer of skin to which the sun creams are applied are dead,[12] it is judged prudent to minimise generation of hydroxyl radicals by surface treatment.[13]

The measurement of coating integrity has presented problems for many years.[14] Chemical analysis cannot differentiate between effective encapsulation, formation of a patchy coating, or bulk precipitation.[7] High resolution transmission electron microscopy (TEM) provides valuable information about the integrity of coatings on individual particles but suffers from problems of statistical unreliability—there are over 10^{13} crystals in 1 g of TiO_2 pigment. The problem is even more acute for the ultrafine crystals used in inorganic sun blocks—the contrast is then insufficient for the coating to be differentiated under normal magnifications. Electrophoretic mobility measurements can detect the gross changes resulting from the surface treatment[7,8,15] but, because of their nature, can only detect bare patches if they are bigger than the double-layer thickness. The coatings are too thin to allow clear results from surface analytical techniques such as ESCA[14,16] and the particulate nature of the titanium dioxide substrate nullifies the normal way of increasing surface sensitivity by increasing the take-off angle.[17] In the particular case of dense silica coatings, selective dissolution experiments have been used to probe the integrity of the coating,[3,7,8] but this method cannot be used to give quantitative estimates of surface coating integrity, nor is it applicable to other coatings *e.g.* of alumina.

Although gaseous dinitrogen is normally IR inactive, adsorbed nitrogen can in specific cases give rise to an IR absorption close to the stretching frequency, measured by Raman spectroscopy, for gaseous nitrogen. For nitrogen adsorbed on supported metals the IR absorption in the region of 2230 cm^{-1} has been assigned to nitrogen molecules adsorbed at coordinatively unsaturated surface sites.[18–20] For nitrogen adsorbed on zeolites the IR absorption is associated with physically adsorbed molecules perturbed by the strong electrostatic fields that exist within the zeolitic cavity.[21] It is probable the IR absorption of nitrogen adsorbed on zinc oxide and titanium dioxide[22] is also associated with strong perturbation of the electrostatic fields associated with these oxide surfaces. By contrast, nitrogen adsorption on silica does not give rise to IR absorption,[20] and on alumina the absorption is vanishingly weak.[23]

We have sought to use these differences in this study of titania coated with increasing amounts of either silica or alumina. We have first examined the effect of the relatively well understood silica coatings and then extended our study to the less understood alumina coatings. Finally we have related our conclusions on the integrity of these coatings to the results of measurements of photocatalytic activity for propan-2-ol oxidation.[9]

Table 1 Description of materials, surface treatment, crystallite size (measured by X-ray line broadening) and resulting surface areas

Sample	Sample origin	Surface area 1[a]/ $m^2\ g^{-1}$	Surface area 2[b]/ $m^2\ g^{-1}$	Surface treatment	Crystallite size/nm
A	Rutile A, uncoated rutile	130	140	None	7
B	Degussa P25	50	50	None	25
C	Aerosil, silicon oxide	200	—	None	—
D	Alon C, aluminium oxide	100	—	None	—
E	Silica-coated rutile A	130	135	0.5% dense silica	—
F	Silica-coated rutile A	100	130	2.3% dense silica	—
G	Silica-coated rutile A	100	105	8.9% dense silica	7
H	Silica-coated rutile A	60	60	20% dense silica	—
I	Alumina-coated rutile A	110	140	7.5% hydrous aluminium oxide	—
J	Alumina-coated rutile A	100	135	15% hydrous aluminium oxide	—
K	Alumina-coated rutile A	100	105	30% hydrous aluminium oxide	—

[a]BET surface areas (1) were measured after outgassing the samples at 110 °C. [b]Surface areas (2) were measured after outgassing the samples at 350 °C.

Experimental

Sample preparation

The powders used in this study are listed in Table 1. Sample A is an experimental material prepared by hydrolysis of $TiCl_4$ and made available by Dr. G. P. Dransfield of Uniqema, Solaveil. Samples E–K were all prepared from the same batch of sample A parent material. Samples E–H were prepared by Iler's 'dense silica' method.[3] A silica coating was applied to a 30 g dm^{-3} dispersion of sample A in water at pH 9. The slurry was heated to 90 °C and to the vigorously stirred suspension the required quantity of sodium silicate and sulfuric acid were added separately but simultaneously at a controlled pH of 9.0. After addition of the required amount of silicate, the pH was adjusted to 6.5 before the suspension was filtered, washed and dried in air at 110 °C.[3,7,8] Samples I–K were prepared by precipitation of alumina onto a 30 g dm^{-3} dispersion of sample A in water. After heating the stirred suspension to 50 °C a set quantity of sodium polyphosphate was added. An addition of aluminium sulfate was made at a controlled pH of 3.0. Caustic sodium aluminate was added at a controlled pH of 10. After addition of the coating reagents, the resulting dispersion was neutralised using sodium hydroxide solution, filtered, washed, and dried in air at 110 °C. Samples of B, C and D are commercial samples prepared by flame hydrolysis of the corresponding chlorides and were kindly provided by Dr. K. Deller of Degussa AG.

Surface areas by gravimetric adsorption of N_2, (σ = 0.162 nm^2) were measured, on a McBain spring balance after outgassing at either 110 °C, (16 h) or for a further 2 h at 350 °C.

IR measurements of adsorbed nitrogen

Disc preparation and pre-treatment. Titanium dioxide powder (0.15–0.20 g) was pressed into a 20 mm self-supporting disc using a SPECAC™ die, at a pressure of 2000 kg cm^{-2}. Prior to pressing, discs of paper were placed above and below the sample to prevent the powder adhering to the die. The discs were carefully transferred to the IR cell shown in Fig. 1. This cell is similar to that described by Egerton and Sheppard[20] and allowed samples to be evacuated at temperatures up to 350 °C. Low temperature measurements were made using liquid nitrogen in the coolant chamber. The cell design allowed rapid thermal equilibrium between the refrigerant and the sample, as measured by a thermocouple placed with its junction in the gas phase near to the centre of the disc. With liquid nitrogen in the coolant chamber and gaseous nitrogen in the cell the indicated temperature was –150 °C.

The IR cell was evacuated to a pressure of 5×10^{-3} kPa. The temperature was then raised to 250 ± 2 °C and the disc was oxidised for 1 h by admitting 13 kPa of oxygen into the isolated system. The oxidised samples were evacuated at 350 °C for 10 h, at 10^{-3} kPa, to remove adsorbed water from the surface prior to nitrogen adsorption. Then the furnace was switched off and the samples allowed to cool naturally.

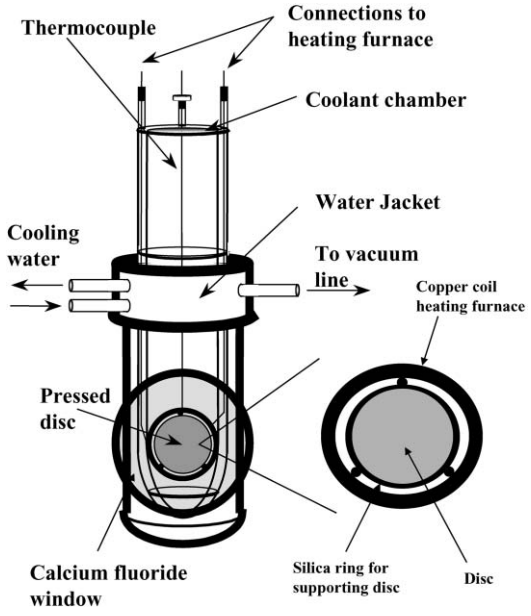

Fig. 1 Schematic showing design of the IR cell.

Spectra of adsorbed nitrogen. Samples were cooled to ~–150 °C by addition of liquid nitrogen to the coolant chamber and were equilibrated for 1 h, to ensure a constant temperature had been reached, prior to recording the first spectrum, using a Bio-Rad FTS40 IR spectrometer. A single beam reference spectrum between 1000 and 4000 cm^{-1} at 256 scans, 2 cm^{-1} resolution was first recorded. Nitrogen pressure in the cell was then increased at regular pressure steps from 0.1 to 9.3 kPa. After each pressure step, samples were equilibrated for 15 min and a fresh single beam spectrum was recorded. Spectra were then referenced to the initial single beam spectrum and recorded as absorbance spectra.

Measurements of photoactivity by propan-2-ol oxidation

Photoactivity measurements. The photocatalytic activity of both uncoated and coated samples was determined by measuring the photogeneration of acetone by a dispersion of TiO_2 in propan-2-ol. Dispersions were prepared by hand stirring 0.4 g of sample with 50 ml of propan-2-ol. The reaction was carried out in a cylindrical Pyrex vessel, (Fig. 2) illuminated, from the base, by two Philips PL-L 36W 09 actinic lamps

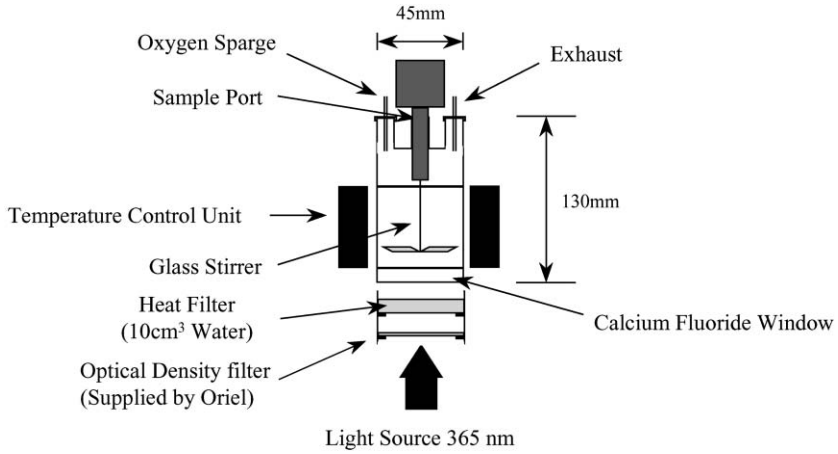

Fig. 2 Schematic of the reactor used for photo-oxidation studies.

placed horizontally in a light box. Radiation from this light box was emitted through a circular port, passed through a Pyrex heat filter and focused on the bottom of the reaction vessel. The relative wavelength distribution of the lamp immediately 'above' the heat filters was measured at 1 nm intervals using a 10 nm slit width, with a Spex 740A Radiometer and is shown in Fig. 3. Cell temperature was controlled by mounting the reactor in a closely fitting cylindrical heater.

Prior to reaction, the vessel was equilibrated at 30 °C and sparged with a constant flow of oxygen. During the reaction the dispersion was continuously stirred and a flow of oxygen was slowly bled across the dead volume. Samples of the reaction mixture were withdrawn by a hypodermic syringe through a sampling port fitted with a septum cap and they were then passed through a 0.2 μm PTFE filter to remove titanium dioxide. They were analysed for acetone content using a Cambridge GC94 gas chromatograph (Chromosorb wax 60/80 mesh at 70 °C) previously calibrated with mixtures of acetone and propan-2-ol using a diethyl ether internal standard, Straight line calibration plots (R^2 0.997) were obtained.

Results

IR nitrogen adsorption results

Adsorption of nitrogen was studied on the nine titania samples given in Table 1. Preliminary experiments on samples A and B confirmed the presence of a band at 2335 cm^{-1}, which increased in intensity with increasing pressure of nitrogen. (Fig. 4) The spectra of adsorbed nitrogen on samples A and B are shown in Fig. 5, which also shows the spectrum of $^{15}N_2$. This absorption can be assigned to molecularly adsorbed dinitrogen on the basis of (a) its correspondence with the Raman stretching frequency of gas phase N_2 at 2331 cm^{-1} and (b) the 77 cm^{-1} measured isotope shift, (Fig. 5) which agrees well with 79 cm^{-1} calculated.

Fig. 6, shows the effect of outgassing temperature on the intensity of the 2335 cm^{-1} band as a function of pressure, for sample A. Based on these results, an outgassing temperature of

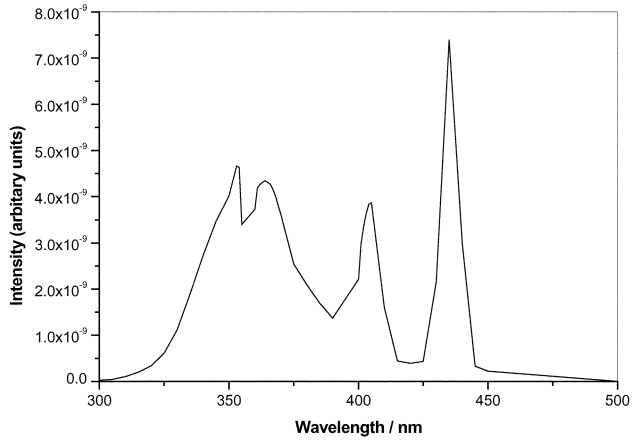

Fig. 3 Relative intensity of radiation from Philips PL-L 09 36W 09 actinic lamps measured with a Spex 740A radiometer.

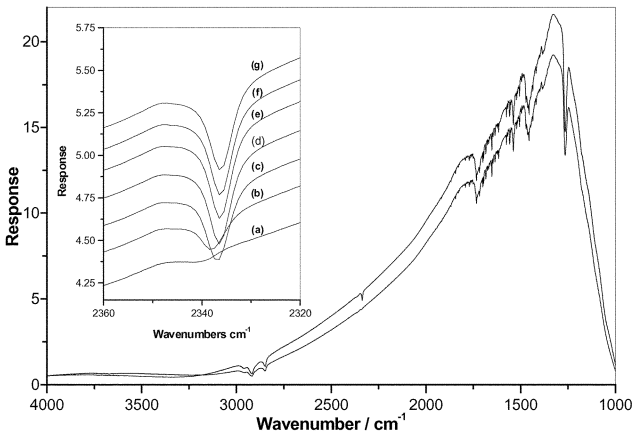

Fig. 4 Single beam spectrum, 2 cm^{-1} sensitivity of N_2 on high area rutile, sample A, before (lower spectrum) and after (upper spectrum) adsorption of N_2. (The bands in the CH stretching region are artefacts due to grease vapour condensed on the windows and are present in the blank spectrum.)The inset shows an enlargement of the 2320–2360 cm^{-1} region of the spectrum at: (a) 0; (b) 1; (c) 1.5; (d) 2.7; (e) 4.9; (f) 6.8; and (g) 9.7 kPa of N_2.

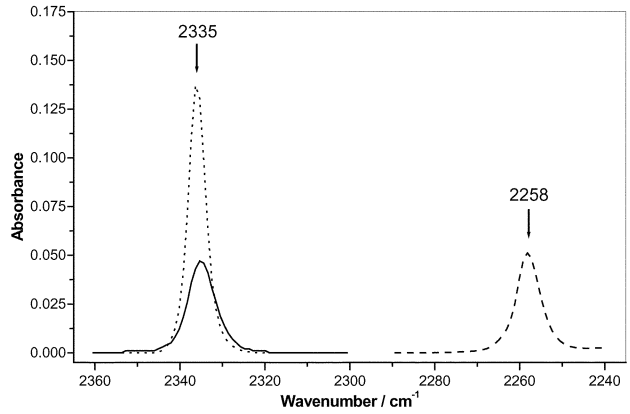

Fig. 5 IR spectra of $^{14}N_2$ adsorbed on high area rutile, sample A — and Degussa P25, sample B - - - - - -. $^{15}N_2$ adsorbed on sample A – – –. Spectra were recorded at −150 °C. Pressures of $^{14}N_2$ and $^{15}N_2$ used were 0.18 kPa and 0.2 kPa, respectively.

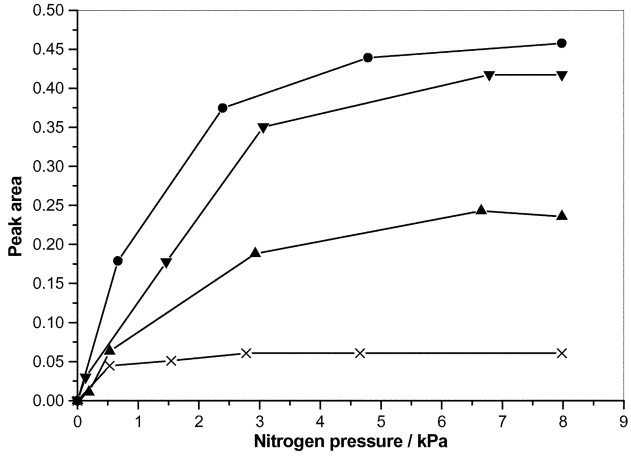

Fig. 6 Effect of outgassing temperature on integrated absorbance of N_2 on rutile sample A. Sample outgassed at: ×, 200 °C; ▲, 250 °C; ▼, 300 °C; ●, 350 °C.

350 °C was chosen for subsequent experiments, as intensities would then be insensitive to small variations in outgassing temperature.

Nitrogen adsorption was then repeated on silicon oxide sample C and aluminium oxide sample D outgassed at 350 °C. The results, given in Fig. 7, demonstrate the absence of an IR band for nitrogen adsorbed on either silicon oxide or aluminium oxide. Further adsorption experiments were then carried out using the silica-coated titania samples E–H.

The IR absorption of nitrogen adsorbed on silica-coated rutile was identical with that of nitrogen on pure rutile except that the bands were weaker. Fig. 8, shows the reduction in IR-active nitrogen at 8 kPa N_2 pressure, on silica-coated TiO_2 at increasing silica levels. Simple calculations, based on a coherent skin of density 2.1 g cm^{-3} applied to identical 10 nm diameter spheres of density 4.2 g cm^{-3}, suggest that, to a first-order approximation, 15% silica would be necessary to form a 0.5 nm coating on the 140 m^2 g^{-1} of high area rutile sample A. If we assume that nitrogen adsorbed on a 0.5 nm silica skin, like N_2 on silica, is IR inactive, the least amount of silica coating required to eliminate the nitrogen band would be 15%. The results in Fig. 8, show that 10% silica is sufficient to reduce the nitrogen band to 20% of the value for uncoated rutile, in broad agreement with the conclusions from the simple model. (The model assumes that IR-active sites are evenly distributed across the titania surface, that the molar absorption coefficient of IR-active nitrogen on rutile is independent of coverage,[22]

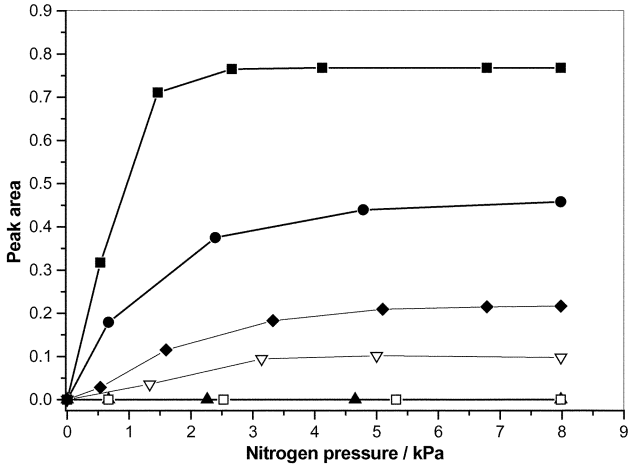

Fig. 7 Nitrogen adsorption isotherms on rutile, sample A ●; Degussa P25, sample B ■; Aerosil, sample C □; Alon C, sample D ▲; silica-coated rutile, sample G ∇; and alumina-coated rutile, sample J ◆; outgassed at 350 °C.

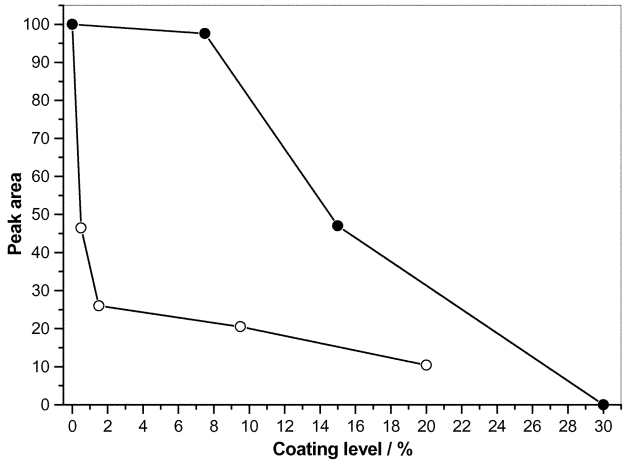

Fig. 8 Decrease in nitrogen peak area with increasing levels of silica coating ○ and hydrous aluminium oxide coating ●. Peak areas were calculated at 8 kPa of nitrogen.

and that IR-inactive nitrogen adsorbed on silica does not affect the molar absorption coefficient of IR-active nitrogen adsorbed on nearby titania.) However, it is remarkable that 0.5% dense silica coating, corresponding to only 5% surface coverage, gives a 50% decrease in the intensity of the nitrogen band. This will be considered further in the Discussion section.

The experiment was then repeated for alumina-coated titanium dioxide, samples I–K and the results are shown in Fig. 8. Once again the only change in the IR absorption due to nitrogen was that at a given pressure the absorptions were weaker.

Photoactivity results

Preliminary experiments confirmed that formation of acetone by oxidation of propan-2-ol required both UV irradiation and TiO_2 catalyst as shown by, *e.g.*, Rudham and co-workers.[9]

Fig. 9, shows rates m^{-2} of acetone formation on samples A–Z at 8 g dm^{-3} of TiO_2. In all cases good straight line plots were obtained.

The variation of acetone formation rate with coating shown in Fig. 10, demonstrates that both silica and alumina coatings reduce the rate of propan-2-ol oxidation. The higher the coating level the larger the reduction. At a fixed coating level, silica reduces photoactivity more effectively than alumina. This is consistent with technological experience of coherent silica layers. 10% silica coating reduces acetone formation to *ca.* 1% of the value for uncoated rutile—qualitatively consistent with the simple model. Significantly, as with the nitrogen band, half of this reduction is achieved at very low coating levels corresponding to only 5% coverage of the rutile surface.

Discussion

Nitrogen adsorption on uncoated titanium dioxide

The IR absorption of adsorbed nitrogen, (Fig. 5) was observed at 2335 cm^{-1} on both the high area rutile, sample A, and on the mainly anatase, Degussa P25, sample B, and agrees well with the peak at 2337 cm^{-1} reported by Onishi *et al.*,[22] although we did not observe the very weak high frequency absorption at 2345 cm^{-1} reported by those workers. Fig. 6 shows that, as the pre-treatment temperature is raised from 200 °C to 350 °C the band intensity increases by ~10 even though the BET area derived from the total nitrogen adsorption changes by less than 10% when the outgassing temperature is increased from 110 to 350 °C. The simplest interpretation of this difference is that IR-active nitrogen is adsorbed only on specific sites on the

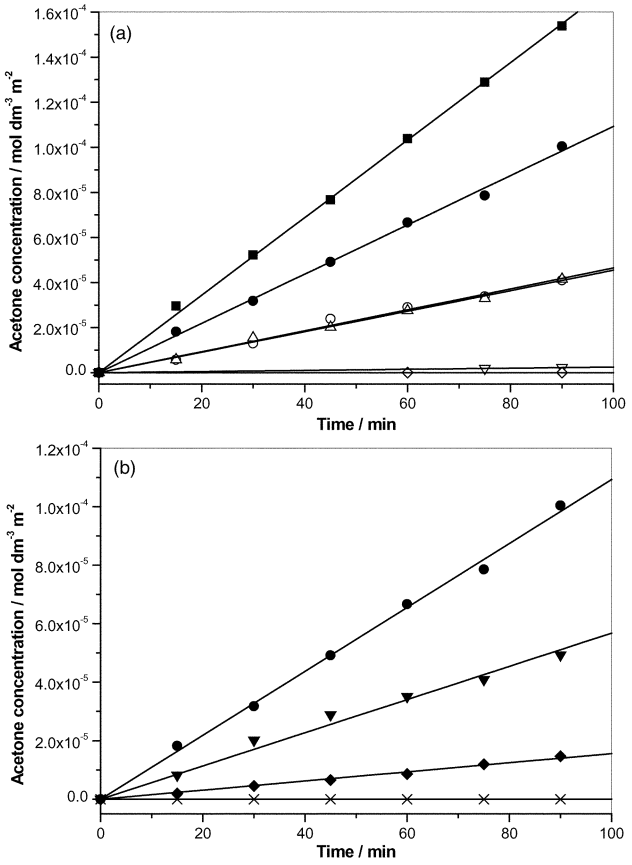

Fig. 9 Graph showing the rate of formation of acetone. a: ● High area rutile, sample A; ■ Degussa P25, sample B; ○ 0.5% silica-coated rutile, sample E; Δ 2.3% silica-coated rutile, sample F; ▽ 8.9% silica-coated rutile, sample G and ◇ 20% silica-coated rutile, sample H. b: ● High area rutile, sample A; ▼ 7.5 % hydrous aluminium oxide coated rutile, sample I; ◆ 15% hydrous aluminium oxide coated rutile, sample J; × 30% hydrous aluminium oxide coated rutile, sample K.

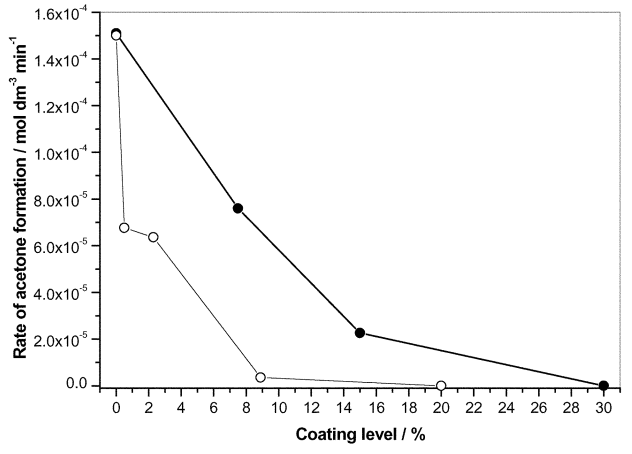

Fig. 10 Dependence of acetone formation rate on coating level for increasing levels of silica coating ○ and hydrous aluminium oxide coating ●.

titanium dioxide surface, and that these sites are blocked by residual water at low outgassing temperatures.

Further, a comparison of the gravimetric adsorption on sample A with the spectroscopic isotherm of IR-active nitrogen on the same sample, Fig. 11, demonstrates that the IR-active nitrogen approaches saturation at a relative pressure at which the gravimetrically determined nitrogen has reached a coverage of only ~0.1. (To compensate for differences in adsorption temperatures both isotherms are plotted as a function of the

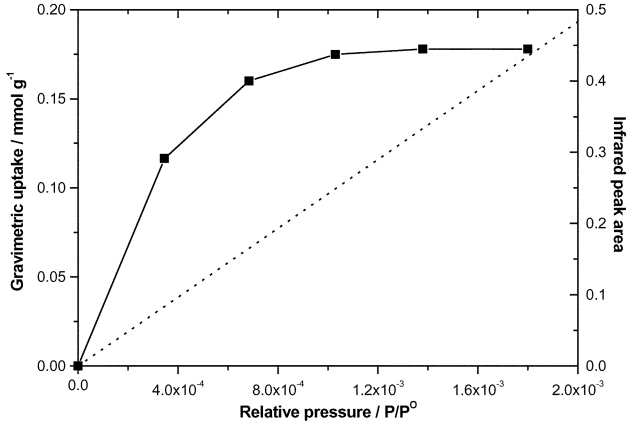

Fig. 11 Comparison of nitrogen adsorption, - - - - - - - (gravimetrically) and nitrogen IR intensity, ■.

relative pressure P/P^{o}, where P^{o} is the saturated vapour pressure of nitrogen at the temperature of the experiment.) This shows that both IR-inactive and IR-active nitrogen can exist on the surface and suggests that the specific sites responsible for IR-active nitrogen account for only *ca.* 10% of the available TiO_2 surface.

The interpretation is supported by the quantitative comparison of adsorption on samples A, 140 m^2 g^{-1}, and B, 50 m^2 g^{-1}. The saturated capacity of IR-active nitrogen, estimated from a Langmuir plot, *i.e.* by plotting equilibrium pressure/peak intensity *versus* pressure, suggested that the number of adsorption sites for IR-active nitrogen is 1.7 times less for A than for B, despite the greater area of A. On a unit area basis the band intensity for B is nearly 5 times as high as for A. Similar variations in intensity between various samples were reported by Onishi *et al.*,[22] but since the present study is primarily concerned with the effect of increasing the inorganic coating on a particular TiO_2 sample A, we have not sought further to identify the cause of these variations, *e.g.* by comparing samples of pure anatase and pure rutile of different morphologies. However, it seems probable that the IR-active nitrogen is associated with surface sites at which a particularly high electrostatic field induces sufficient polarisation of adsorbed nitrogen to make the adsorbed species IR active. At low outgassing temperatures these sites are probably blocked by adsorbed water molecules.

Nitrogen adsorption on silica-coated titanium dioxide

XRD line broadening confirmed that no change in the crystallite size of the rutile crystals occurred as a result of coating. Silica coatings deposited in the manner used for these samples are believed to be essentially non-porous. Iler[3,7,24] has demonstrated that a silica coating of this type can form an essentially non-porous and continuous (*i.e.* non-patchy) shell around a titanium dioxide core and that such shells significantly reduce dissolution of the titanium dioxide in concentrated HCl. Similarly, Mulvaney *et al.*[25] have demonstrated that colloidal particles of gold coated with dense silica are not attacked by cyanide ions. However, since progressive attack of a core may occur through a small fraction of bare patches, neither of these methods allows the fractional coverage to be quantitatively assessed.

Fig. 8, shows that a silica coating greatly reduces the IR absorption at 2335 cm^{-1} and that the band intensity falls approximately linearly as the coating level increases from 3 to 20%. Extrapolation suggests that a coating level of 30% (0.2% m^{-2} of substrate surface) would eliminate the sites responsible for the IR-active surface species. Since nitrogen adsorbed on Aerosil silica is not IR active, the simplest interpretation is that 30% silica is sufficient to completely cover the TiO_2 surface and

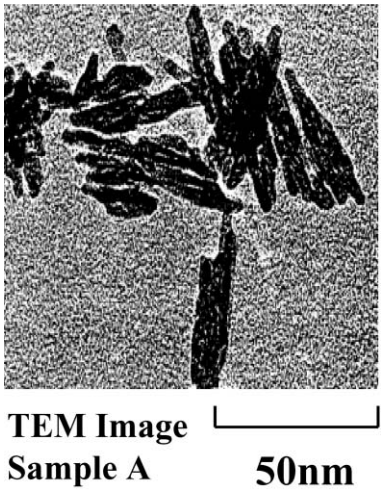

Fig. 12 High magnification TEM of high area rutile, sample A, showing acicularity of the crystals. The bar represents 100 nm.

that at lesser levels of coating the IR absorption is of nitrogen adsorbed on uncoated patches. The difference between 30% deduced in these experiments and the estimate of 15% earlier in the paper may be associated with the approximate nature of the calculation—*e.g.* electron micrographs, such as Fig. 12, show that the uncoated rutile is not spherical but consists of aggregates of lenticular particles. Therefore, to the extent that adsorption sites responsible for IR-active nitrogen are distributed evenly across the titania surface, this study suggests that the IR band of adsorbed nitrogen measures the amount of residual uncoated TiO_2.

Significantly, a 0.5% silica coating, ~2% of the amount estimated for elimination of the nitrogen band, reduces its intensity by 50%. Most probably, the distribution of active sites on the TiO_2 surface is not completely even and initially the silica tends to deposit on those areas of surface with a high concentration of active sites.

However, we also note that the high magnification electron micrographs show agglomerates of cylindrical or lenticular particles and suggest that the surface area is made up of external area and internal area. Comparison of nitrogen adsorption on the high area rutile with lower area, non-porous samples, Fig. 13, shows that the initial adsorption on the high area rutile is relatively greater than on the non-porous rutile, consistent with adsorption in the micropores between particles. The initial deposition of silica may be disproportionately effective by blocking access to the internal surface as shown in Fig. 14. (This model appears to disagree with the negligible change in measured surface area caused by the initial deposition of silica, but it is difficult estimate the surface area of partially coated composite particles.) Subsequent deposition of silica would coat the external area of the particles and cause the observed, slower, decrease in nitrogen band intensity.

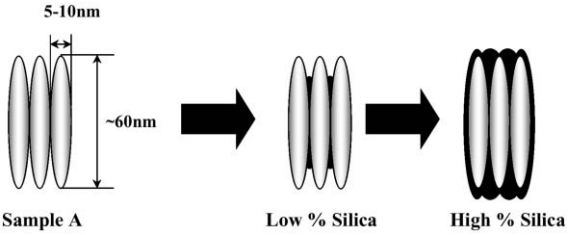

Fig. 14 Diagrammatic representation of suggested successive stages in the coating of sample A with silica.

Nitrogen adsorption on alumina-coated titanium dioxide

The decrease in nitrogen band intensity with increasing alumina coating is also shown in Fig. 8. A 30% coating eliminates the nitrogen adsorption, in good agreement with the 30% estimate for silica. However, unlike silica, low-alumina coatings have relatively little effect on the nitrogen band intensity. Evidently low levels of alumina, unlike silica, neither preferentially block sites for adsorption of IR-active nitrogen nor cap the pores.

Dependence of propan-2-ol oxidation rates on coating

Fig. 10, demonstrates that coating rutile with either silica or alumina decreases the rate of photo-oxidation of propan-2-ol to acetone. Silica coatings, which more efficiently masked the sites responsible for IR-active nitrogen, more effectively reduce propan-2-ol oxidation. Plots of photocatalytic activity *versus* coating level, (Fig. 10) mirror the plots of nitrogen intensity *versus* coating level, (Fig. 8). A graph of propan-2-ol oxidation rate as a function of the intensity of the nitrogen band, Fig. 15, demonstrates the close relationship between photoactivity and IR-active sites. Therefore it is reasonable to suppose that the inorganic coating has reduced the rate of generation of the catalytically active hydroxyl radicals, and that the sites responsible for IR-active nitrogen are either the same as, or closely connected with, the sites responsible for the generation of catalytically active hydroxyls.

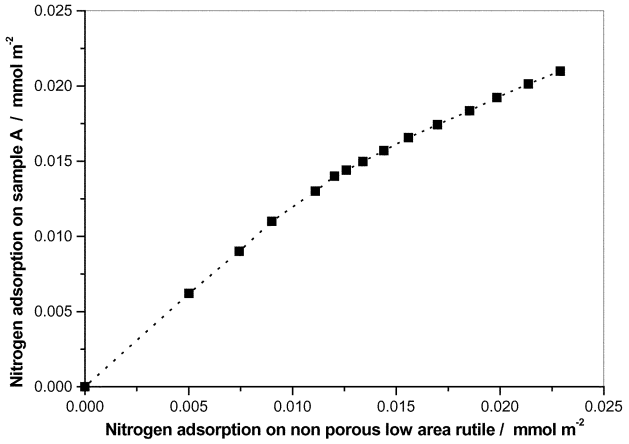

Fig. 13 Comparison of nitrogen adsorption on sample A *versus* nitrogen uptake on non-porous low area rutile, at corresponding nitrogen pressure.

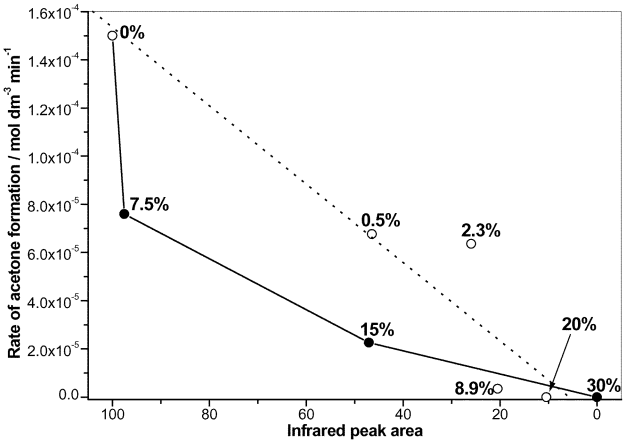

Fig. 15 Rate of change of acetone formation measured by propan-2-ol oxidation *versus* IR peak area for increasing levels of silica (○) and hydrous aluminium oxide (●) coating on sample A.

Conclusions

Nitrogen adsorbed on titanium dioxide can be IR active. The proportion of adsorbed nitrogen that is IR active is different on samples A and B, suggesting that the given IR-active adsorbed nitrogen is associated with specific sites on the TiO_2 surface. The intensity of the band near 2331 cm^{-1} may be used to monitor the proportion of IR-active sites that remain accessible to N_2 in TiO_2 samples that have been coated with silica or alumina, since nitrogen adsorbed on silica and alumina is not IR active. For both silica- and alumina-coated samples the decrease in IR-active nitrogen on coating is roughly mirrored by the decrease in photoactivity measured by propan-2-ol oxidation. However, the correlation is better for dense silica coatings than for alumina. In the case of alumina, $\leqslant 7\%$ coating has little effect on nitrogen adsorption, (Fig. 8) but a significant effect on propan-2-ol oxidation, (Fig. 10). We speculate that this may be because the alumina coating is porous to nitrogen but not to propan-2-ol. Despite this, the plot of photoactivity *versus* nitrogen intensity is linear for coating levels from 7 to 30%.

Acknowledgement

The work was carried out as part of an EPSRC, CASE award with Solaveil business of Uniqema. The authors thank Dr G. P. Dransfield, Dr L. Kessell, and Mrs S. Cutter, (Solaveil) for helpful discussion and supply of sample. We also thank Dr P. A. Christensen, (Newcastle) for providing spectroscopic facilities and for his sustained advice and help.

References

1 T. A. Egerton, *Kirk Othmer Encyclopedia of Chemical Technology*, John Wiley & Sons, Inc., New York, 1997, vol. 24, pp. 225–274.
2 V. P. S. Judin, *Chem. Br.*, 1993, 503.
3 R. K. Iler, to E. I. du Pont de Numours. *U.S. Pat.*, 2 885 366, 1959..
4 P. B. Howard and G. D. Parfitt, *Croat. Chem. Acta*, 1977, **50**, 15.
5 M. J. B. Franklin, K. Goldsbrough, G. D. Parfitt and J. Peacock, *J. Paint Technol.*, 1970, **42**, 740.
6 U. Gesenhues, *J. Colloid Interface Sci.*, 1994, **168**, 428.
7 T. A. Egerton, *KONA Powder Particle*, 1998, **16**, 46.
8 P. Mulvaney, L. M. Liz-Marzan, M. Giersig and T. Ung, *J. Mater. Chem.*, 2000, **10**, 1259.
9 R. B. Cundall, R. Rudham and M. S. Salim, *J. Chem. Soc., Faraday Trans. 1*, 1976, **72**, 1642.
10 H. Swartz, K. J. Liu, T. Walczak, T. Panz, M. Kobayashi and W. Zavadoski, *J. Cosmet. Sci.*, 1998, **49**, 125.
11 P. A. Christensen, A. Dilks, T. A. Egerton and J. Temperley, *J. Mater. Sci.*, 1999, **34**, 5689.
12 J. Knowlton and S. Pearce, *Handbook of Cosmetic Science and Technology*. Elsevier Science, Amsterdam, 1993.
13 M. A. Mitchnick, N. Y. Wainscott, A. J. O'Lenick and G. Lilburn, *U.S. Pat., 5 756*, **788**, 1998.
14 Y. M. Cross and J. Dewing, *Surf. Interface Anal.*, 1979, **1**, 26.
15 D. N. Furlong, K. S. W. Sing and G. D. Parfitt, *J. Colloid Interface Sci.*, 1979, **69**, 356.
16 R. E. Day and T. A. Egerton, *Colloids Surf.*, 1987, **23**, 137.
17 T. A. Egerton, G. D. Parfitt, Y. Cheug and D. P. Wightman, *Colloids Surf.*, 1983, **7**, 311.
18 R. P. Eischens and J. Jacknow, *Proc. 3rd Int. Cong. Catal.*, Book of Conference Proceedings, North Holland, Co., 1965, p. 627.
19 R. Van Hardeveld and A. Van Montfoort, *Surf. Sci.*, 1966, **4**, 396.
20 T. A. Egerton and N. Sheppard, *J. Chem. Soc., Faraday Trans. 1*, 1974, **70**, 1357.
21 E. Cohen de Lara and Y. Delaval, *J. Chem. Soc., Faraday Trans. 2*, 1986, **74**, 790.
22 Y. Sakata, N. Kinoshita, K. Domen and T. Onishi, *J. Chem. Soc., Faraday Trans. 1*, 1987, **83**, 2765.
23 H. P. Wang and J. T. Yates Jr, *J. Phys. Chem.*, 1984, **88**, 852.
24 R. K. Iler, *The Chemistry of Silica*, Wiley, New York, 1979.
25 L. M. Liz-Marzán, M. Giersig and P. Mulvaney, *Langmuir*, 1996, **12**, 4329.